Bandpass Filter for 5G Sub-6 GHz Bands

Jiajia Wang[1], Shuo Yu[1], Xiaofan Yang[2], and Xiaoming Liu[1, 3, *]

[1] *The School of Physics and Electronic Information, Anhui Normal University, Wuhu 241002, China*
[2] *The State Key Laboratory of Complex Electromagnetic Environment Effects on Electronic and Information System, Luoyang, Henan, China*
[3] *Anhui Provincial Engineering Center on Information Fusion and Control of Intelligent Robot, Wuhu 241002, China*

ABSTRACT: The performance requirements for filters in the microwave frequency band are particularly stringent, particularly in terms of high bandwidth and out-of-band rejection. However, meeting these requirements within the constraints of a compact size presents a significant challenge. A coupled step-impedance resonator bandpass filter is proposed. The filter combines U-shaped branches and L-shaped branches to create multiple resonance points while expanding the bandwidth, and the in-band ripple is also improved by this folded structure that greatly reduces the filter size. The microstrip filter measures only $9.6\,\text{mm} \times 8.8\,\text{mm} \times 1.1\,\text{mm}$, has a center frequency of 4.65 GHz, and achieves a relative bandwidth of 60.2%. The filter can be used in 5G n77 ($3300 \sim 4200\,\text{MHz}$), n78 ($3300 \sim 3800\,\text{MHz}$), n79 ($4800 \sim 4960\,\text{MHz}$), and WLAN ($5150 \sim 5850\,\text{MHz}$) bands. In addition, the filter has a left-side rectangular coefficient of 1.12, insertion loss $< 0.4\,\text{dB}$, and return loss better than 17 dB.

1. INTRODUCTION

The 5G communication technology has rapidly evolved in recent years. The 5G spectrum is divided into two regions. The first region is located in the range of 450 MHz–6 GHz, this band is referred to as FR1 (Frequency Range 1), also known as Sub-6 GHz. The second region is located in the range of 24.25 GHz–52.6 GHz and is called FR2 (Frequency Range 2) [1].

With the booming development of the information industry and wireless communication, devices with filtering function are more and more applied to mobile communication technology. 5G communication technology places more stringent requirements on filter performance, such as bandwidth, edge roll off, insertion loss and compactness [2]. In order to increase communication capacity and avoid interference between adjacent channels, filters are required to have steep out-of-band rejection. To improve the signal-to-noise ratio, a low insertion loss in the filter passband is preferred. In order to meet the trend of miniaturization of modern communication terminals, filters are required to have a smaller size.

To meet these requirements, many methods and structures have been proposed, such as step impedance resonator (SIR) [3–5], combined resonator [6–11], ring resonator [12–14], and parallel coupled line reference [15, 16]. The main transmission line structures used in conventional microwave filters are: microstrip lines [17, 18], waveguides [19–21], and coaxial lines [22–24]. A bandpass filter with two pairs of anti-parallel hybrid coupled step impedance resonators was proposed in [7]. Although the filter is compact, its bandwidth is not sufficiently wide. A method for designing bandpass filters using resonators was proposed in [9]. However, the 3 dB bandwidth is only 12.9%, making its practical application

less preferred. A novel dual-mode dielectric waveguide (DW) filter with controlled transmission zeros was proposed in [20]. In [23], a novel folded bandpass filter in an empty substrate integrated coaxial line (ESICL) technique is described. However, these two filters are large in size, complex, and not conducive to process. Waveguide filters and coaxial filters are significantly larger, more expensive to process and less easy to integrate with other planar devices. Therefore, microstrip filters bear advantages of low cost and ease of integration in comparison with other methods.

In this paper, a bandpass filter based on a step impedance resonator is proposed. The filter is structurally simple and compact, with a main structure of two U-shaped branches and two L-shaped branches, which expands the bandwidth and improves the stability of the filter by creating multiple resonance points. The microstrip filter can cover 5G n77 ($3300 \sim 4200\,\text{MHz}$), n78 ($3300 \sim 3800\,\text{MHz}$), n79 ($4800 \sim 4960\,\text{MHz}$) and WLAN ($5150 \sim 5850\,\text{MHz}$) bands simultaneously. In addition, the filter has good steep roll off on the left single side, insertion loss $< 0.4\,\text{dB}$, return loss better than 17 dB, good in-band rejection and flat in-band ripple, and can be widely used in wireless communication systems.

The rest of the paper is structured as follows: Section 2 describes the design of the filter; Section 3 describes the current distribution of the filter; Section 4 belongs to the parametric analysis of the filter; Section 5 belongs to the measurements and discussion; and Section 6 concludes this work.

2. FILTER DESIGN

The geometry of this bandpass filter is shown in Fig. 1. The dielectric substrate is copper-clad TP-2 ($\varepsilon_r = 10.2$ and $\tan \delta \le 1 \times 10^{-3}$), domestically produced microwave laminated dielectric copper-clad substrates in China with a thickness of 1.1 mm.

---

* Corresponding author: Xiaoming Liu (xiaoming.liu@ahnu.edu.cn).

The dimensions of this bandpass filter are only $8.8\,\text{mm} \times 9.6\,\text{mm}$. To evaluate the performance of this filter, simulations were performed using ANSYS HFSS. Table 1 lists the values of parameters for the final design.
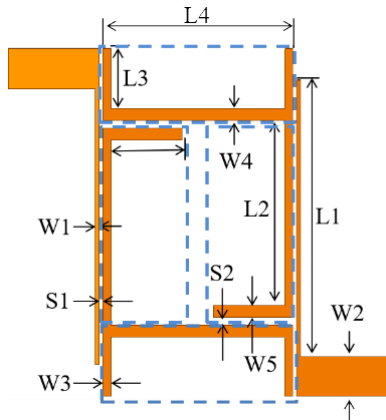

FIGURE 1. Diagram structure of the filter.

TABLE 1. Dimensions of the proposed filter (unit: mm).

Parameter	Value	Parameter	Value
$L1$	7	$W1$	0.1
$L2$	4.7	$W2$	1
$L3$	1.5	$W3$	0.2
$L4$	4.8	$W4$	0.3
$L5$	1.8	$W5$	0.3
$S1$	0.1	$S2$	0.2

The evolution of the filter is shown in Fig. 2. The filter uses multiple branches to create resonance and thus generate the operating band, shown as Filter.1 in Fig. 2. Then, $L2$ is extended to form a U-shaped branch, labeled Filter.2. The U-shaped branches are marked in dashed rectangular area. Next, a rectangular branch is added to make an L-shaped branch as indicated with rectangular lines, labeled Filter.3. Lastly, extension of $L1$ forms the final structure, which is labeled as Filter.4. To demonstrate the filter evolution process, the simulation results are plotted in Fig. 3.

The initial structure of the filter is Filter.1, which has an open rectangular frame and two rectangular branches. As can be seen from the simulation results in Fig. 3, Filter.1 produces transmission poles at 3.74 GHz and 6.63 GHz, and transmission zeros at 6.1 GHz, and steep-edge steepening on the high-frequency side. However, its insertion loss and return loss are not sufficiently good. And even worse, the bandwidth is not wide enough. In order to improve the resonance effect and improve the quality of the passband, Filter.2 is designed. Although one more resonance point is added, only the higher frequency part is improved.

Further improvement is made as Filter.3. Obviously, it can be seen from Filter.3 in Fig. 3 that the addition of the $L6$ branch will generate another resonance point and thus significantly improve the resonance effect of the entire operating band, ultimately improving the passband performance and producing an operating band of 3.35 to 6.26 GHz. Since the passband range

does not completely cover the n78 band, Filter.3 needs to be further improved. By extending $L1$, the bandwidth is enlarged to cover the 5G n77, n78, n79 and WLAN bands.

3. CURRENTS DISTRIBUTION

To more clearly illustrate the process of resonance generation, the surface current distribution is plotted as shown in Fig. 4. The current distributions at frequencies of 3.47 GHz, 4.52 GHz, and 5.79 GHz are shown in Figs. 4(a), (b), (c), respectively.

In Fig. 4(a), the open rectangular frame is colored in dark red and brings together the main current distribution, indicating that the open rectangular frame produces the first resonance point at 3.47 GHz. The resonant frequency of the filter is determined by the length of the resonant element, which can be calculated according to the following equation.

$$f_0 = c / \left(\lambda_g \sqrt{\varepsilon_{eff}} \right) \qquad (1)$$

where c represents the speed of light; ε_{eff} represents the effective dielectric constant; and the wavelength λ_g can be calculated using Eq. (2):

$$\lambda_g = (L4 - W3 + L2) \qquad (2)$$

Substituting each parameter into Eq. (1), the resonant frequency reads as 3.41 GHz, which is very close to the simulation value. Repeating the analysis for 4.52 GHz, λ_g can be calculated by Eq. (3):

$$\lambda_g = 4 (L5 + L2 + W4 + W5) \qquad (3)$$

Substituting Eq. (3) into Eq. (1), the calculated resonant frequency is 4.53 GHz, which is almost the same as the simulated one. Similar analysis is conducted for 5.79 GHz, as shown in Fig. 4(c), and the main currents are distributed at the L-shaped U-shaped branches, which indicates that the combination of these structures can generate a third resonance. Calculated by Eq. (4) and substituted into Eq. (1), the corresponding frequency is found to be 5.76 GHz.

$$\lambda_g = 4 (L3 + L5 + L5) \qquad (4)$$

The calculation results of the three resonance points are compared with the final simulation results. Only the calculation results of the first resonance point have a relatively large error with the simulation results, but the calculation and simulation results of the other two resonance points are in good agreement. Current distribution is an efficient way assisting the filter design.

4. PARAMETRIC STUDY

In order to further obtain the optimal performance, the main parameters $L1$, $L2$, $L3$, $L4$, and $L5$ were parametrically analyzed.

Due to the coupling between the U-shaped and L-shaped structures, parameters $L1$, $L2$, $L3$, $L4$, and $L5$ have a significant impact on the overall performance of the filter. From Fig. 5, it can be seen that the bandwidth of the filter becomes wider when the values of $L1$, $L2$, $L3$, and $L4$ are increased; the bandwidth of the filter becomes narrower when the values of $L1$, $L2$, $L3$, and $L4$ are decreased; and the opposite is true for
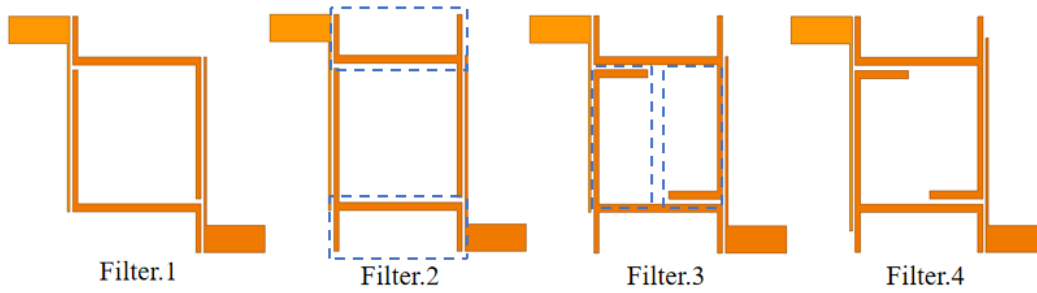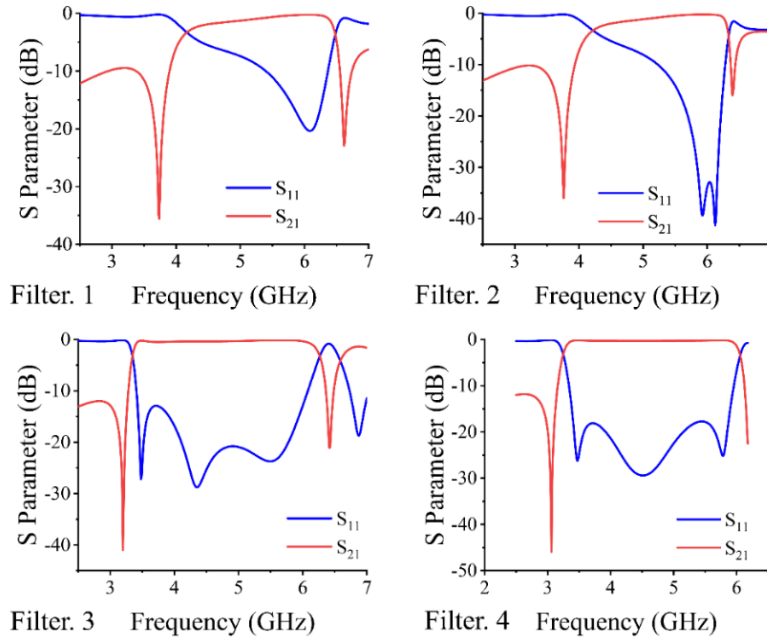
FIGURE 2. Evolution of the proposed filter.

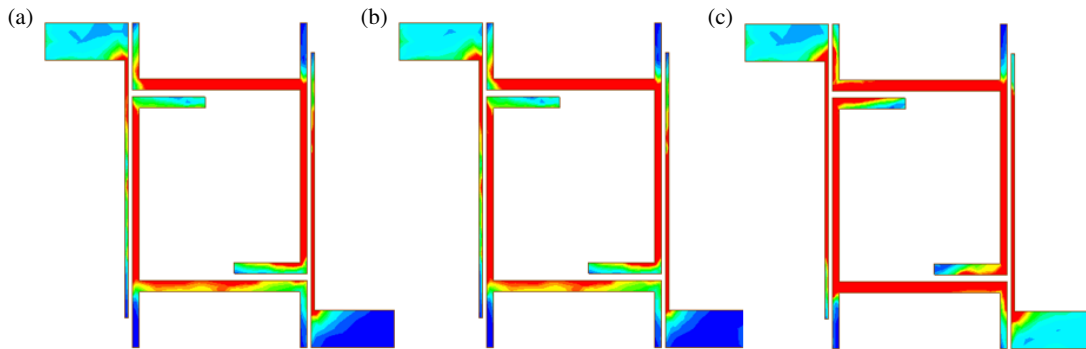**FIGURE 3**. S-parameter simulation results of Filter.1–Filter.4.

FIGURE 4. Current distribution of the filter. (a) 3.47 GHz; (b) 4.52 GHz; (c) 5.79 GHz.

the value of $L5$. As the values of these parameters decrease, the operating band of the filter is shifted to high frequencies, making the passband range not fully cover the 5G n78 band, while as the values of these parameters increase, the operating band of the filter is shifted to low frequencies. In addition, increasing the values of $L1$, $L2$, and $L5$ will make the resonance of the

filter worse, and increasing the values $L3$ and $L4$ will reduce the return loss of the filter.

From the parameter study, it is clear that these parameters have an effect on the operating band of the filter as well as the resonance effect. The change of parameters all lead to the frequency deviation. In comparison, $L4$ has the greatest effect on
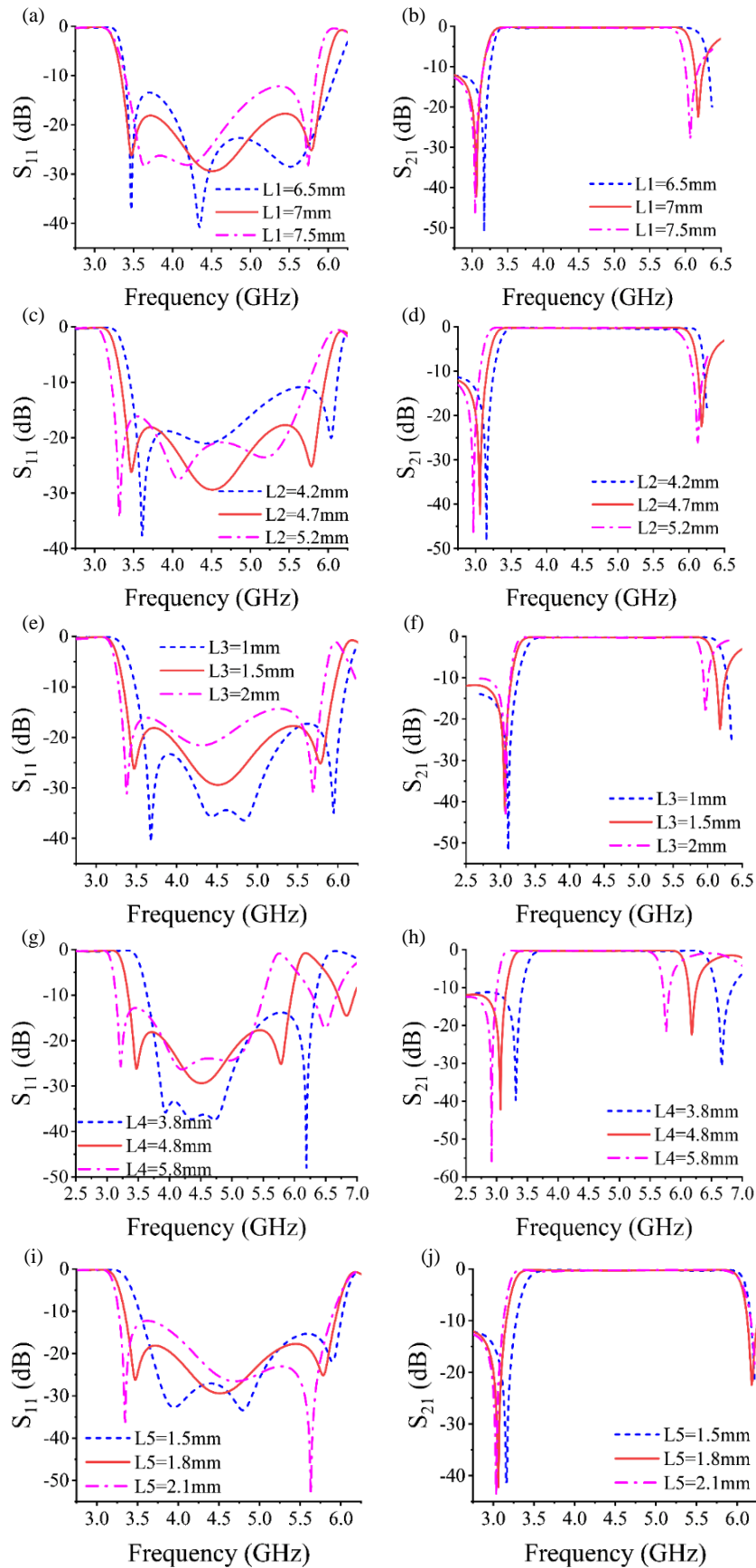
FIGURE 5. Parameter study for (a) $L1$ S_{11}; (b) $L1$ S_{21}; (c) $L2$ S_{11}; (d) $L2$ S_{21}; (e) $L3$ S_{11}; (f) $L3$ S_{21}; (g) $L4$ S_{11}; (h) $L4$ S_{21}; (i) $L5$ S_{11}; (j) $L5$ S_{21}.
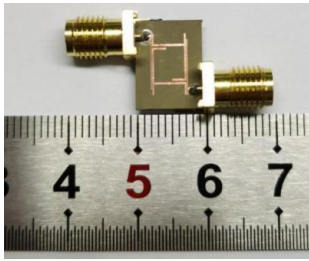
FIGURE 6. Photo of the fabricated filter.

FIGURE 7. S-parameter measurement using a vector network analyzer.
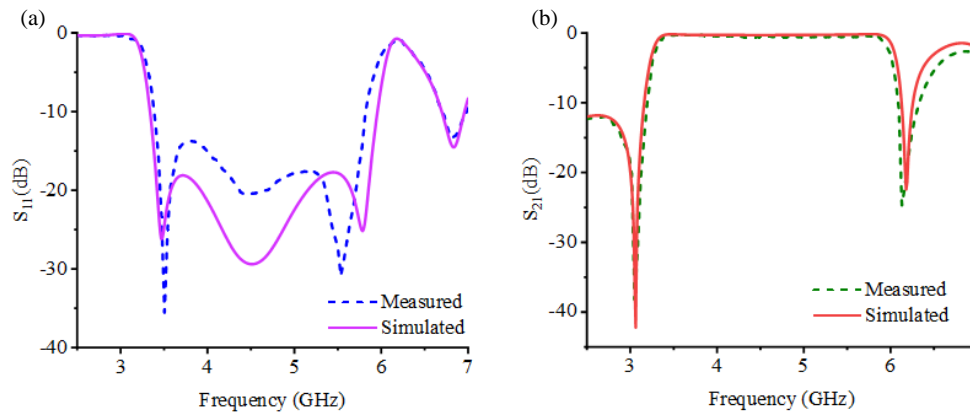

FIGURE 8. Comparison between simulation and measurement of (a) S_{11}, (b) S_{21}.

the passband frequency deviation, and $L2$ has the greatest effect on the resonance effect.

5. MEASUREMENT AND DISCUSSION

It is demonstrated that the performance of the designed filter is satisfactorily good in simulation. The fabricated filter is shown in Fig. 6.

The S-parameters of the filter were measured using a vector network analyzer, as shown in Fig. 7. The measurements were performed on an AV3672D VNA in the frequency range of 2–7 GHz. Two cables are connected to the VNA and then calibrated using a conventional Short-Load-Open-Thru (SLOT) method. After calibration, the filter is fixed to the sub-miniature version A (SMA) connector. Then, S_{11} and S_{21} of the filter are measured.

From Fig. 8, it can be seen that the simulated results of S_{21} are in good agreement with the measured ones, and although the simulated results of S_{11} have a slight deviation from the measured results, it is not the essential parameter of the filter in the paper. These frequency bands, such as n77 ($3300 \sim 4200$ MHz), n78 ($3300 \sim 3800$ MHz), n79 ($4800 \sim 4960$ MHz) and WLAN ($5150 \sim 5850$ MHz), are still the operating frequency bands for the filter.

In process, the accuracy of PCB manufacture is an important cause of errors. On the other hand, the dielectric parameters of the substrate are affected by environment. It could also be a possible reason for the discrepancy between experimental and simulated results.

A comparison of the single-band filters is shown in Table 2. As can be seen, the filter size is compact, and there is a significant increase in filter bandwidth compared to $[5, 7, 9, 23, 26, 28, 29]$. In addition, the insertion loss is lower than $[9, 25, 27, 29]$, and the return loss is better than $[7, 9, 25, 28]$. In short, the filter has several advantages. First, the filter has a wide bandwidth to be used in the 5G Sub 6G and WLAN bands, and can be widely used in wireless communication system. Second, the filter has a compact structure, small size, low insertion loss, good in-band rejection, and flat in-band ripple. Third, the filter has several advantages of microstrip filter, easy processing, easy integration, low cost, and can be widely used in wireless communication system. In

TABLE 2. Comparison of the single-band filter to the designs in the literature.

Filter	Filter size (mm^2)	FBW	IL (dB)	RL (dB)
[5]	40×20.4	4.5%	< 1.5	> 16
[7]	9×6	4.9%	< 2.2	> 12
[9]	14×17	47%	< 0.6	> 12
[23]	52.3×53.9	2%	< 3.14	> 15
[25]	46.6×30.7	53.1%	< 0.9	> 12
[26]	32.4×28.8	12%	< 1.2	> 13
[27]	30.3×17.1	62.4%	< 0.9	> 14.5
[28]	22.7×22.7	8.2%	< 2.7	> 11
[29]	11.7×9.5	25.8%	< 1.02	> 25
This work	9.6×8.8	60.2%	< 1.1	> 13

addition, the filter rectangular coefficient is 1.12, and the filter has a good attenuation steepness [4, 8, 9, 24, 30]. In summary, this bandpass filter is overall a satisfactory design suitable for wireless communication.

6. CONCLUSION

The microstrip filter proposed in this paper has a simple and compact structure, and the coupled step-impedance resonator bandpass filter is realized by using U-shaped branches and L-shaped branches structures, which makes the filter performance more stable, and the size is greatly reduced. The bandpass filter was tested for the 5G Sub-6 GHz band. The test results show that the insertion loss is < 1.1 dB, and the return loss is better than 13 dB, which can meet the applications in 5G n77 (3300 ∼ 4200 MHz), n78 (3300 ∼ 3800 MHz), n79 (4800 ∼ 4960 MHz) and WLAN (5150 ∼ 5850 MHz) bands.

ACKNOWLEDGEMENT

REFERENCES

[1] Sim, C.-Y.-D., H.-D. Chen, J. Kulkarni, J.-J. Lo, and Y.-C. Hsuan, "Recent designs to achieving wideband MIMO antenna for 5G NR sub-6 GHz smartphone applications," in *2020 International Symposium on Antennas and Propagation (ISAP)*, 417–418, Jan. 2021.

[2] Mateu, J., Y. Yusuf, R. Perea-Robles, J. C. C. Gómez, A. Gimenez, P. M. Iglesias, and R. Aigner, "Acoustic wave transversal filter for 5G N77 band," *IEEE Transactions on Microwave Theory and Techniques*, Vol. 69, No. 10, 4476–4488, Oct. 2021.

[3] Qin, W., J. Cai, Y.-L. Li, and J.-X. Chen, "Wideband tunable bandpass filter using optimized varactor-loaded SIRs," *IEEE Microwave and Wireless Components Letters*, Vol. 27, No. 9, 812–814, Sep. 2017.

[4] Sheikhi, A., A. Alipour, and A. Mir, "Design and fabrication of an ultra-wide stopband compact bandpass filter," *IEEE Transactions on Circuits and Systems II: Express Briefs*, Vol. 67, No. 2, 265–269, Feb. 2020.

[5] Zakharov, A., S. Rozenko, L. Pinchuk, and S. Litvintsev, "Microstrip quazi-elliptic bandpass filter with two pairs of antiparallel mixed-coupled SIRs," *IEEE Microwave and Wireless Components Letters*, Vol. 31, No. 5, 433–436, Mar. 2021.

[6] Zakharov, A., S. Rozenko, and M. Ilchenko, "Varactor-tuned microstrip bandpass filter with loop hairpin and combline resonators," *IEEE Transactions on Circuits and Systems II: Express Briefs*, Vol. 66, No. 6, 953–957, Jun. 2019.

[7] Dong, G., S. Li, and X. Yang, "A tunable bandpass filter with extended passband bandwidth," *International Journal of Microwave and Wireless Technologies*, Vol. 14, No. 10, 1233–1240, 2022.

[8] Liu, Q., J. Wang, G. Zhang, L. Zhu, and W. Wu, "A new design approach for balanced bandpass filters on right-angled isosceles triangular patch resonator," *IEEE Microwave and Wireless Components Letters*, Vol. 29, No. 1, 5–7, Jan. 2019.

[9] Khater, M. A., P. Adhikari, M. Thorsell, S. Gunnarsson, B. Edward, and D. Peroulis, "Bandpass filter with tunable/switchable in-band interference rejection," *IEEE Microwave and Wireless Components Letters*, Vol. 31, No. 10, 1115–1118, Oct. 2021.

[10] Li, L.-P., W. Shen, J.-Y. Ding, and X.-W. Sun, "Compact 60-GHz on-chip bandpass filter with low insertion loss," *IEEE Electron Device Letters*, Vol. 39, No. 1, 12–14, Jan. 2018.

[11] Sekiya, N., "Design of compact and high-power HTS double-strip dual-mode patch resonator filter for transmit filter applications," *IEEE Transactions on Applied Superconductivity*, Vol. 27, No. 4, 1–4, 2016.

[12] Li, J., Y. Zhan, W. Qin, Y. Wu, and J.-X. Chen, "Differential dielectric resonator filters," *IEEE Transactions on Components, Packaging and Manufacturing Technology*, Vol. 7, No. 4, 637–645, Apr. 2017.

[13] Jiang, D., Y. Liu, X. Li, G. Wang, and Z. Zheng, "Tunable microwave bandpass filters with complementary split ring resonator and liquid crystal materials," *IEEE Access*, Vol. 7, 126 265–126 272, 2019.

[14] Zhang, T., M. Tian, Z. Long, M. Qiao, and Z. Fu, "High-temperature superconducting multimode ring resonator ultrawideband bandpass filter," *IEEE Microwave and Wireless Components Letters*, Vol. 28, No. 8, 663–665, Aug. 2018.

[15] Gopal, B. G. and V. Rajamani, "Design of X band parallel coupled line BPF by analytical approach," *Analog Integrated Circuits and Signal Processing*, Vol. 96, No. 3, 469–474, Sep. 2018.

[16] Ma, M., F. You, T. Qian, C. Shen, R. Qin, T. Wu, and S. He, "A wide stopband dual-band bandpass filter based on asymmetrical parallel-coupled transmission line resonator," *IEEE Transactions on Microwave Theory and Techniques*, Vol. 70, No. 6, 3213–3223, Jun. 2022.

[17] Cheng, T. and K.-W. Tam, "A wideband bandpass filter with reconfigurable bandwidth based on cross-shaped resonator," *IEEE Microwave and Wireless Components Letters*, Vol. 27, No. 10, 909–911, Oct. 2017.

[18] Gómez-Garcia, R., J.-M. Muñoz-Ferreras, and D. Psychogiou, "High-order input-reflectionless bandpass/bandstop filters and multiplexers," *IEEE Transactions on Microwave Theory and Techniques*, Vol. 67, No. 9, 3683–3695, Sep. 2019.

[19] Ebadi, S. M., J. Örtegren, M. S. Bayati, and S. B. Ram, "A multipurpose and highly-compact plasmonic filter based on metal-insulator-metal waveguides," *IEEE Photonics Journal*, Vol. 12, No. 3, 1–9, Jun. 2020.

[20] Huang, Z., Y. Cheng, and Y. Zhang, "Dual-mode dielectric waveguide filters with controllable transmission zeros," *IEEE Microwave and Wireless Components Letters*, Vol. 31, No. 5, 449–452, May 2021.

[21] Wang, F., V. F. Pavlidis, and N. Yu, "Miniaturized SIW bandpass filter based on TSV technology for THz applications," *IEEE Transactions on Terahertz Science and Technology*, Vol. 10, No. 4, 423–426, Jul. 2020.

[22] Tamiazzo, S., G. Macchiarella, and F. Seyfert, "A true in-line coaxial-cavity filter with two symmetric zeros," *IEEE Microwave and Wireless Components Letters*, Vol. 31, No. 6, 666–669, Jun. 2021.

[23] Martinez, L., A. Belenguer, V. E. Boria, and A. L. Borja, "Compact folded bandpass filter in empty substrate integrated coaxial line at S-band," *IEEE Microwave and Wireless Components Letters*, Vol. 29, No. 5, 315–317, May 2019.

[24] Zhang, Z.-C., S.-W. Wong, X. Yu, B. Zhao, D. Wang, and R. Chen, "Compact quadruple-mode wideband bandpass filter using L-shaped feed-line in a single cavity," *IEEE Microwave and Wireless Components Letters*, Vol. 31, No. 10, 1111–1114,

Oct. 2021.

[25] Li, D. and K.-D. Xu, "Multifunctional switchable filter using coupled-line structure," *IEEE Microwave and Wireless Components Letters*, Vol. 31, No. 5, 457–460, May 2021.

[26] Marín, S., J. D. Martínez, C. I. Valero, and V. E. Boria, "Microstrip filters with enhanced stopband based on lumped bisected PI-sections with parasitics," *IEEE Microwave and Wireless Components Letters*, Vol. 27, No. 1, 19–21, Jan. 2017.

[27] Narayane, V. B. and G. Kumar, "A selective wideband bandpass filter with wide stopband using mixed lumped-distributed circuits," *IEEE Transactions on Circuits and Systems II: Express Briefs*, Vol. 69, No. 9, 3764–3768, Sep. 2022.

[28] Liang, C., Y. Liu, T. Liu, and F. Tai, "Bandpass filter design using quad-mode stub-loaded loop resonator," in *2019 International Applied Computational Electromagnetics Society Symposium-China (ACES)*, Vol. 1, 1–2, Aug. 2019.

[29] Rao, Y., J. Zhou, H. J. Qian, and X. Luo, "Compact cross-coupled bandpass filter with wide stopband and low radiation loss using SIDGS," in *2021 IEEE MTT-S International Microwave Filter Workshop (IMFW)*, 30–32, Nov. 2021.

[30] Zhu, Y.-Y., Y.-L. Li, and J.-X. Chen, "A novel dielectric strip resonator filter," *IEEE Microwave and Wireless Components Letters*, Vol. 28, No. 7, 591–593, Jul. 2018.